Acta Crystallographica Section B
**Structural Science**
ISSN 0108-7681

# Location of the H atoms in ammonium persulphate by deuteron NMR. Verification by X-ray diffraction

**Thorsten Schmidt,[a] Heike Schmitt,[a] Herbert Zimmermann,[a] Ulrich Haeberlen,[a]* Zdzisław T. Lalowicz,[b] Zbigniew Olejniczak[b] and Thomas Oeser[c]**

[a]Max-Planck-Institut für Medizinische Forschung, AG Molekülkristalle, Jahnstraße 29, 69120 Heidelberg, Germany, [b]Institute of Nuclear Physics, ul. Radzikowskiego 152, 31342 Krakow, Poland, and [c]Organisch-Chemisches Institut der Universität Heidelberg, Im Neuenheimer Feld 270, 69120 Heidelberg, Germany

Correspondence e-mail: ulrich.haeberlen@mpimf-heidelberg.mpg.de

Received 22 April 2002
Accepted 24 June 2002

It is demonstrated that H atoms can be located by the spectroscopic method of deuteron NMR. The requirement is that the 'heavy-atom' positions are known from diffraction studies. The technique allows an accuracy of the order of 0.01 Å. The compound studied is ammonium persulphate (APS), $(NH_4)_2S_2O_8$. APS crystallizes in space group $P2_1/n$ with lattice parameters $a = 6.1340\ (2)$, $b = 7.9324\ (3)$, $c = 7.7541\ (3)$ Å and $\beta = 94.966\ (1)^\circ$ at $T = 118$ K. In perdeuterated crystals of APS, only one of the deuterons of every $ND_4^+$ ion becomes localized at low temperatures. Therefore, most of this work uses samples with 9% deuteration. In such crystals, most of the ammonium ions containing deuterons come in the form of $NDH_3^+$ ions. At $T < 25$ K, the single deuteron of these ions becomes localized in one of four equilibrium sites. The deuteron site occupancies differ from each other and are measured at 17 K. The deuterons are located in three steps. (i) The deuteron quadrupole-coupling (QC) tensors are measured at 17 K. Their unique principal directions are identified, as is well justified, with the N—D bond directions. (ii) The fine structure of a deuteron NMR line is analyzed in terms of the magnetic dipole–dipole interactions between all nuclei in an $NDH_3^+$ ion to obtain the N—D and D—H internuclear distances. (iii) An empirical relation between deuteron QC constants and D···O distances in N—D···O hydrogen bonds is exploited to assign the N—D bond vectors to the appropriate N atom of which there are four in the unit cell. The results are highly relevant for an understanding of the complex tunnelling and stochastic reorientation dynamics of the ammonium ions in APS. They are verified by a complementary X-ray diffraction study.

## 1. Introduction

The structure of ammonium persulphate (APS), $(NH_4)_2S_2O_8$, was solved during the pre-computer infancy of X-ray diffraction (Zachariasen & Mooney, 1934). The H atoms were not mentioned. In 1969, when computers had become available, the structure of APS was reinvestigated and refined by Sivertsen & Sørum (1969). This time, the H atoms were mentioned. In difference maps, maxima in the neighborhood of the N atoms were found and ascribed to the H atoms. These maxima were, however, too diffuse to warrant an attempt to locate the H atoms.

In this work, which actually is the first step of a study of the dynamics, including rotational tunnelling, of fully and partially deuterated ammonium groups in APS, we use deuteron NMR to determine the directions of all N—D bonds. The basis of the method is the well tested proposition that the unique principal direction of the nearly axially symmetric electric-field gradient (EFG) tensor **V** at the site of a deuteron is parallel, with

© 2002 International Union of Crystallography
Printed in Great Britain – all rights reserved

deviations of less than 1°, to the covalent bond of that deuteron (Schmitt *et al.*, 2001). The unique principal direction is that of approximate axial symmetry. The principal directions of the EFG tensors at the locations of the deuterons can be measured by deuteron NMR with considerable precision. The deuteron NMR resonances of sparsely deuterated crystals of APS display a well resolved fine structure for selected orientations of the applied magnetic field **B** relative to the sample crystal. The analysis of this fine structure enables us to determine the *lengths* of the N—D bonds. What remains to be done to locate the H atoms is to assign the deuteron bond vectors to one of the four N atoms in the unit cell. To solve this problem, we draw on an empirical rule (Blinc, 1976) that relates the quadrupole-coupling constant QCC of a deuteron involved in an N—D···O hydrogen bond to the D···O distance. The approach leads to a convincing solution of the assignment problem and completes the location of the H atoms in APS.

The task is relevant, we think, because of the fascinating classical and quantum-mechanical (tunnelling) dynamics that isotopically pure and mixed ammonium ions undergo in APS. These dynamics have been studied extensively by various methods (Clough *et al.*, 1991; Lalowicz *et al.*, 1997; Schmidt, 1999; Kankaanpää *et al.*, 2001). As will become clear below, they are intimately linked to the positions of the H atoms in APS and to the hydrogen bonds that are formed by some but not all of the deuterons/protons.

The level of independence of prior knowledge is different for the location of H atoms by NMR and for the determination of the directions of the N—D bond vectors. The latter task requires only prior knowledge of the unit cell (monoclinic symmetry; $a$, $b$, $c$; $\beta$). The former requires, in addition, knowledge of the N-atom positions that play the role of anchors for the N—D bond vectors. At the beginning of this work, these positions were available only at room temperature (Sivertsen & Sørum, 1969). Combining room- and low-temperature information as we do is a procedure that may be questioned. Therefore, we made a (successful) effort to check our NMR results with modern X-ray diffraction. Because one central aspect of this work is the deuteron NMR method as such, we strive to give a seamless account of its logic.

## 2. Background information and initial considerations

The primary quantity that is determined in a deuteron NMR experiment is the deuteron quadrupole-coupling tensor $\mathbf{Q} = (2eQ/3h)\mathbf{V}$, where $e$, $\mathbf{Q}$ and $h$ are, respectively, the elementary charge, the nuclear quadrupole moment ($Q_{\rm deuteron} = 0.286 \times 10^{-30}$ m$^2$) and Planck's constant. $\mathbf{Q}$ is a traceless symmetric second-rank tensor and its dimension is Hz. Evidently, $\mathbf{Q}$ and $\mathbf{V}$ share a common set of principal axes. The high-field NMR spectrum of deuterons in magnetically equivalent sites consists of a doublet with the separation of the components

$$\Delta\nu_Q = \hat{\mathbf{B}}^{\dagger} \cdot \mathbf{Q} \cdot \hat{\mathbf{B}}, \qquad (1)$$

where $\hat{\mathbf{B}}$ is the unit vector along the static magnetic field $\mathbf{B}$ applied in the NMR experiment. The *proviso* of (1) is that the deuterons are stationary in their sites, small-amplitude vibrations and librations apart. By measuring $\Delta\nu_Q$ for a sufficiently large number $N$ ($N \geq 5$) of different directions $\hat{\mathbf{B}}$ relative to the crystal, one obtains $\mathbf{Q}$ by a straightforward five-parameter fitting procedure (Schmitt *et al.*, 2001).

The space group of APS is $P2_1/c$, $Z = 2$, $a = 7.830$, $b = 8.008$, $c = 9.505$ Å and $\beta = 139.93°$ (Sivertsen & Sørum, 1969). Pairs of ammonium ions are related by inversion centers and are thus magnetically equivalent, leaving us with $2 \times 4$ spectroscopically distinguishable deuterons, which, in turn, are pairwise related by $2_1$ axes. At room temperature, the H atoms of the ammonium ions in APS are exchanging places at a rate $k$ of roughly $10^{11}$ s$^{-1}$, with the result that only an averaged quadrupole-coupling tensor $\mathbf{Q}_{\rm av}$ can be observed. Because of the approximate tetrahedral symmetry of the ammonium ion, $\mathbf{Q}_{\rm av} \simeq 0$. When the temperature of the crystal is lowered, $k$ becomes smaller. However, isotopically pure ions, $NH_4^+$ or $ND_4^+$, never settle in a definite orientation with all four N—D or N—H bonds pointing statically (*i.e.* on a time scale longer than $10^{-3}$ s) in fixed directions. Instead, rotational tunnelling sets in (Clough *et al.*, 1991), meaning that the protons/deuterons become delocalized. Rotational tunnelling in APS is a complex process in as much as the tunnelling frequency $\nu_t$ is 'high' [269 MHz in $NH_4^+$ (Clough *et al.*, 1991) and 1.6 MHz in $ND_4^+$ (Schmidt, 1999)] for tunnelling about one of the four (approximate) $C_3$ axes of the ion, whereas it is 'small' (4 kHz in $ND_4^+$) for another $C_3$ axis and it is virtually zero for the remaining two $C_3$ and all three $C_2$ axes. The spectroscopic consequences of fast tunnelling are that no resonances can be observed that can be assigned to individual deuterons and that the observed doublet splittings cannot be related to a quadrupole-coupling tensor *via* (1). However, the perfect analogy between a rotationally tunnelling (deuterated) methyl group and a *uniaxially* tunnelling $ND_4^+$ ammonium ion allows us to analyze the spectra of $ND_4^+$ ions with expressions for the doublet splittings derived for the methyl group case (Detken *et al.*, 1995, equation 17*ff.*). This analysis provides access to the equilibrium orientations of the $ND_4^+$ groups in APS. This has been calculated by one of us (Schmidt, 1999) and is discussed further below.

To bypass the problem with delocalized deuterons in fully deuterated ammonium groups, we also worked with isotopically diluted samples, that is, crystals of APS with 9% deuteration. In these crystals, most of the deuterons reside in $NDH_3^+$ isotopomers. At low enough temperatures, the deuteron will settle in one of the four equilibrium sites available to it. It will remain there for a time long enough to be considered as static for deuteron NMR purposes. It transpires that the single deuteron in $NDH_3^+$ ions will settle preferentially in the site whose bond defines in $ND_4^+$ or $NH_4^+$ ions the primary tunnelling axis, that is, the $C_3$ axis about which high-frequency rotational tunnelling sets in at low temperatures. We will call this site (bond) the *preferred* site (bond). The direction of the preferred bond can be accessed directly in crystals of both fully and partially deuterated APS. Those

**Table 1**
NMR samples, their rotation axes $\mathbf{d}_{rot}$, reference directions $\mathbf{d}_{ref}$ and reference angles $\phi_{ref}$.

| Sample | Deuteration | $\mathbf{d}_{rot}$ $\vartheta, \varphi$† | $\mathbf{d}_{ref}$ $\vartheta, \varphi$† | $\phi_{ref}$ |
|---|---|---|---|---|
| I | 99.8% | 90°, 270° | 95.9°, 0°‡ | 120.0° |
| II | 99.8% | 156.8°, 103.9° | 95.9°, 0° | 153.5° |
| III | 9% | 62.2°, 43.7°§ | 144.0°, 0°¶ | 108.5° |
| IV | 9% | 90°, 270° | 144.0°, 0° | 171.0° |

† Polar angles in the SO frame with $x \parallel \mathbf{a}$, $y \parallel \mathbf{b}$, $z \parallel \mathbf{c}^*$. ‡ Direction in monoclinic plane that is perpendicular to $\mathbf{d}_{rot}^{II}$. § $\mathbf{d}_{rot}^{III} \parallel (2\mathbf{a} + \mathbf{b} + \mathbf{c})$, which is a pronounced zone axis. ¶ Direction in monoclinic plane that is perpendicular to $\mathbf{d}_{rot}^{III}$.

deuterons of $NDH_3^+$ ions that do not go to the preferred site will settle with almost equal probability in any one of the three other equilibrium sites. A 9% deuterated crystal hence contains, with unequal abundance, static deuterons in all equilibrium sites, enabling us to measure the respective quadrupole-coupling tensors and thus to find all the equilibrium N—D bond directions. In order to obtain the situation where all the deuterons of $NDH_3^+$ (and of $ND_2H_2^+$) ions have settled in definite lattice sites, the crystal must be cooled down to a temperature below 25 K. Most of the measurements on which we report were carried out at 17 K. The few $ND_3H^+$ and $ND_4^+$ ions in 9% deuterated samples never settle in a definite orientation; instead, they undergo rotational tunnelling.

## 3. Experimental

Perdeuterated crystals of APS were obtained by repeated recrystallization of isotopically normal APS from a solution in $D_2O$ (99.8%). Similary, crystals of partially deuterated APS were grown from a 95% $H_2O$/5% $D_2O$ solution with the H atoms of the dissolved $(NH_4)_2S_2O_8$ taken into account. The deuteron content of the crystals so obtained was checked by IR and deuteron NMR and transpired to be about 9%. All crystals had well developed natural-growth planes suitable for orientation by optical means.

The (homemade) NMR spectrometer ($|\mathbf{B}| = 11$ T) and the data-analysis procedures are described by Schmitt *et al.* (2001). An Oxford Instruments helium flow cryostat together with a temperature controller, ITC-4, from the same company was used to set the sample temperature at any value down to 5 K and to keep it stable within ±0.1 K. The bulk of the work reported here was performed at 17 K, where the spin-lattice relaxation time $T_1$ is about 30 min. At still lower temperatures, $T_1$ becomes prohibitively long. The NMR probe is equipped with a goniometer that allows the rotation of the sample about an axis perpendicular to the applied field **B**. Its crucial part is a worm drive made of aluminium and Vespel. It is connected with a long rod to a knob outside the cryostat for manual rotation and also to a dial whose finest division corresponds to a 0.1° rotation of the sample. When kept perfectly dry the drive works down to 5 K. For each rotation angle $\phi$ for which a spectrum is taken, the data analysis requires knowledge of the direction of **B** in a crystal fixed frame, for which we choose the so-called standard orthonormal (SO) frame with axes parallel to **a**, **b** and $\mathbf{c}^*$. The direction of **B** can be specified once we know (i) the direction $\mathbf{d}_{rot}$ of the axis about which the crystal is rotated, (ii) the angle $\phi$ and (iii) a reference direction $\mathbf{d}_{ref}$, which is the direction of **B** for a reference rotation angle $\phi_{ref}$. The directions of **B**, $\mathbf{d}_{rot}$, $\mathbf{d}_{ref}$ and other vectors (bond directions) will be specified by their polar coordinates $\vartheta$ and $\varphi$ in the SO frame.

From both the fully and the partially deuterated crystals, we prepared two samples: one with $\mathbf{d}_{rot}$ parallel to **b**, the other for a general rotation axis. The samples were fixed in 5 mm tubes with $\mathbf{d}_{rot}$ parallel to the tube axis. In Table 1 we list for all four samples, labeled I–IV, $\mathbf{d}_{rot}$, $\mathbf{d}_{ref}$ and $\phi_{ref}$. The information about $\phi_{ref}$ and about the sense of $\mathbf{d}_{rot}$ was inferred directly from the NMR data. For $\mathbf{d}_{rot} \parallel \mathbf{b}$, **B** lies for any $\phi$ in the monoclinic plane of the crystal, and the spectra simplify inasmuch as the resonances from pairs of deuterons related by $2_1$ axes coincide. Collecting data, that is, quadrupole splittings $\Delta\nu_Q(\phi)$, from a monoclinic crystal rotated about a single *general* axis is sufficient for the determination of a quadrupole-coupling tensor (Tesche *et al.*, 1993).

## 4. Results

In Fig. 1 we present three deuteron NMR spectra from the fully deuterated sample I, recorded at 70, 40 and 18 K. The 70 K spectrum reflects the high-temperature dynamic situation: the $ND_4^+$ ions are frequently jumping between all 12 equilibrium orientations available to the ions by permution symmetry of like particles. The time-average EFG tensor sensed by each deuteron is close to zero; a single sharp line without quadrupole splitting is observed. An intermediate situation is encountered at 40 K: one deuteron has settled in the preferred site and stays there for intervals longer than, say, 1 ms. It gives rise to the outer of the two doublets and is given the label 4. The three remaining deuterons 1–3 are still rapidly reorienting about the preferred N—D bond and give rise to a

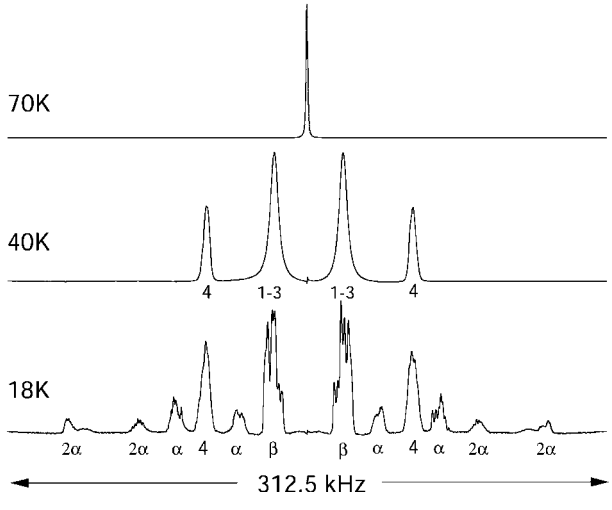


**Figure 1**
Deuteron NMR spectra of the fully deuterated sample I of APS characterizing three dynamic ranges of the ammonium groups. $\phi = 130°$, *cf.* Fig. 5. See text for description.

common doublet whose splitting is one-third of that of the outer one. This ratio of one-third is found for all rotation angles of the sample and provides evidence for (close) tetrahedral symmetry of the $ND_4^+$ ion (Bernhard & Haeberlen, 1991). The 18 K spectrum reflects the low-temperature situation: deuteron 4 in the preferred site still gives rise to a doublet with the same splitting as at 40 K. The other three deuterons undergo uniaxial three-site rotational tunnelling. According to the permutation symmetry (without transpositions) of three identical particles, each librational state of the $-ND_3$ group splits into a totally symmetric $A$ state and two degenerate $E^a$ and $E^b$ states. The energy difference between the $A$ and the $E^{a,b}$ states is the tunnelling frequency multiplied by $h$. The $A$ state contributes 80% to the intensity of the innermost richly structured doublet (the so-called $\beta$-lines), while the $E^a$ and $E^b$ states give rise to the outer small doublets (the so-called $\alpha$- and $2\alpha$-lines) and to 20% of the intensity of the inner doublet. The nomenclature is that of Lalowicz *et al.* (1988). The structure of the $\beta$-lines allows us to infer that the tunnel frequency is 1.6 MHz.

In Fig. 2 we show three spectra of the partially deuterated sample III recorded at 17 K for different rotation angles $\phi$. Note how different these spectra are from the 18 K spectrum of the fully deuterated sample I. In Fig. 2, all doublets arise from identifiable localized deuterons. The $\phi = 64^\circ$ spectrum shows 'many' well resolved doublets, although not as many as are possible in principle (eight). For the $\phi = 108.5^\circ$ spectrum, the rotation angle was carefully adjusted for **B** to be in the monoclinic plane of the crystal. Four doublets are observed, corresponding to the deuterons in sites 1–4 as indicated. The

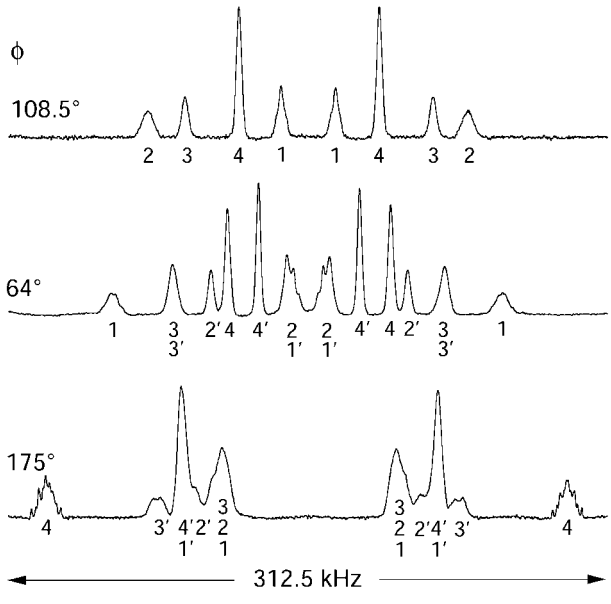


**Figure 2**
Deuteron NMR spectra of the partially deuterated sample III of APS, $T = 17$ K. $\phi = 108.5^\circ$: The magnetic field **B** lies in the monoclinic plane; four doublets are observed. Isotopic ordering is reflected by differing line intensities. Site 4 is the preferred one. $\phi = 64^\circ$: A general orientation of **B**; eight doublets appear in principle, two pairs coincide accidentally. $\phi = 175^\circ$: **B** is nearly parallel to the N—D4 bond. The resonance of D4 is richly structured, *cf.* Fig. 6. It provides information about $r_{ND}$ and $r_{HD}$.

intensity of a line (its area) is a direct measure of the deuteron occupancy of the respective site. Site 4 is obviously the preferred one: 44% of the deuterons are in this site. Sites 2 and 3 are occupied equally (17.5%), while 21% of the deuterons reside in site 1. These site occupancies depend on the temperature. The phenomenon of differing deuteron/proton site occupancies is called isotopic ordering and has been observed before in, for example, aspirin—$CH_2D$ (Schiebel *et al.*, 1999). We show the $\phi = 175^\circ$ spectrum in Fig. 2 because the outermost doublet displays, for this particular rotation angle, a rich well resolved fine structure. This fine structure allows us to deduce the N—D bond length (see below).

We have recorded spectra like those shown in Fig. 1 (samples I and II, $T = 44$ K and 13 K) and in Fig. 2 (samples III and IV, $T = 17$ K) for complete sets of rotation angles $\phi$ and plotted the line positions *versus* $\phi$. In NMR jargon, such plots are called rotation patterns. The rotation patterns of samples II (44 K), III (17 K), IV (17 K) and I (13 K) are shown in Figs. 3–5. We first discuss the 44 K rotation pattern of crystal II. The data shown in Fig. 3 stem exclusively from the deuteron in the preferred site 4 and its monoclinic related partner, which we label by a prime. These deuterons are virtually static at 44 K, and the data in Fig. 3 allow us to extract their quadrupole-coupling tensors $\mathbf{Q}_4$ and $\mathbf{Q}'_4$ and thus to find the preferred N—D bond directions $\mathbf{b}_4$ and $\mathbf{b}'_4$. The first step of the data analysis is to find in Fig. 3 the rotation angle $\phi = \phi_m$ for which **B** is in the monoclinic plane. The obvious condition for this is $\Delta\nu_Q(\phi_m) = \Delta\nu'_Q(\phi_m)$. There are four candidates for $\phi_m$, labeled $A$, $B$, $C$ and $D$ in Fig. 3. $B$ and $C$ can quickly be discarded because a closer inspection reveals that, in fact, $\Delta\nu_Q(\phi_{B,C}) = -\Delta\nu'_Q(\phi_{B,C})$. To find out whether $\phi_m = \phi_A$ or $\phi_m = \phi_D$, we tested both candidates by trying to fit traceless symmetric tensors $\mathbf{Q}_4$ and $\mathbf{Q}'_4$ to the data. Candidate $\phi_A$ leads to a standard deviation $\sigma_A = 47.1$ kHz, which is not acceptable, whereas $\phi_D$ leads to $\sigma_D = 0.71$ kHz, which is excellent. The quality of this fit is actually demonstrated by the full traces in Fig. 3. These traces are of the form $A + B\cos 2(\phi - \phi_0)$, which is the theoretical $\phi$-dependence of

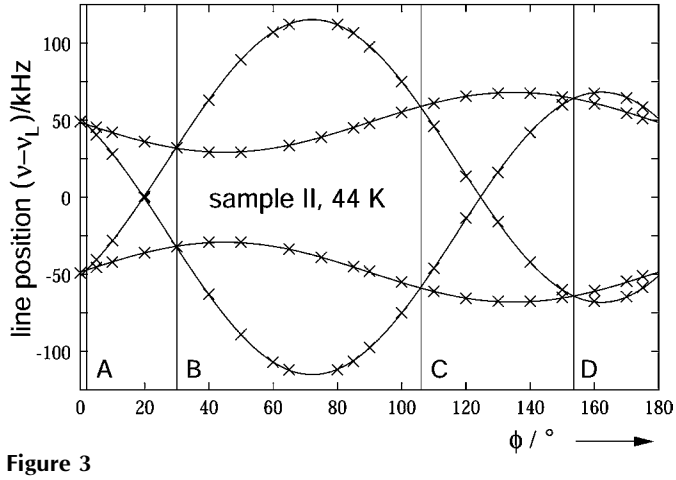


**Figure 3**
Rotation pattern of deuteron NMR line positions of sample II recorded at 44 K. Only the data from the deuterons in the preferred sites 4 and 4′ are shown. These deuterons are localized at 44 K, *cf.* Fig. 1.

deuteron resonance positions (Mehring, 1976). $A$, $B$ and $\phi_0$ are parameters that depend on the particular $\mathbf{Q}$ tensor, the rotation axis $\mathbf{d}_{\rm rot}$ of the sample crystal and the starting angle of the rotation pattern. For the fit, we chose $\mathbf{d}^{\rm II}_{\rm rot}$ as given in Table 1. However, if, in the fit, we reverse the sense of rotation of the crystal, we obtain a result that is equally as good as before, meaning that, at this point, we cannot tell the two cases apart. In terms of the unique principal axes of $\mathbf{Q}_4$ and $\mathbf{Q}'_4$, *i.e.* in terms of the preferred bond directions $\mathbf{b}_4(\vartheta, \varphi)$ and $\mathbf{b}'_4(\vartheta', \varphi')$, the two solutions are:

$(\vartheta, \varphi) = (130.4^\circ, 106.0^\circ)$, $(\vartheta', \varphi') = (49.6^\circ, 74.0^\circ)$ for $\mathbf{d}^{\rm II}_{\rm rot} = (156.8^\circ, 103.9^\circ)$; and

$(\vartheta_{\rm r}, \varphi_{\rm r}) = (132.6^\circ, 84.3^\circ)$, $(\vartheta'_{\rm r}, \varphi'_{\rm r}) = (47.4^\circ, 95.7^\circ)$ for $\mathbf{d}^{\rm II}_{\rm r,rot} = -\mathbf{d}^{\rm II}_{\rm rot}$,

where the index r stands for the *reversed* sense of rotation. Which of the two alternatives is the correct one will become clear when we have analyzed in a similar manner the 17 K data from crystal III.

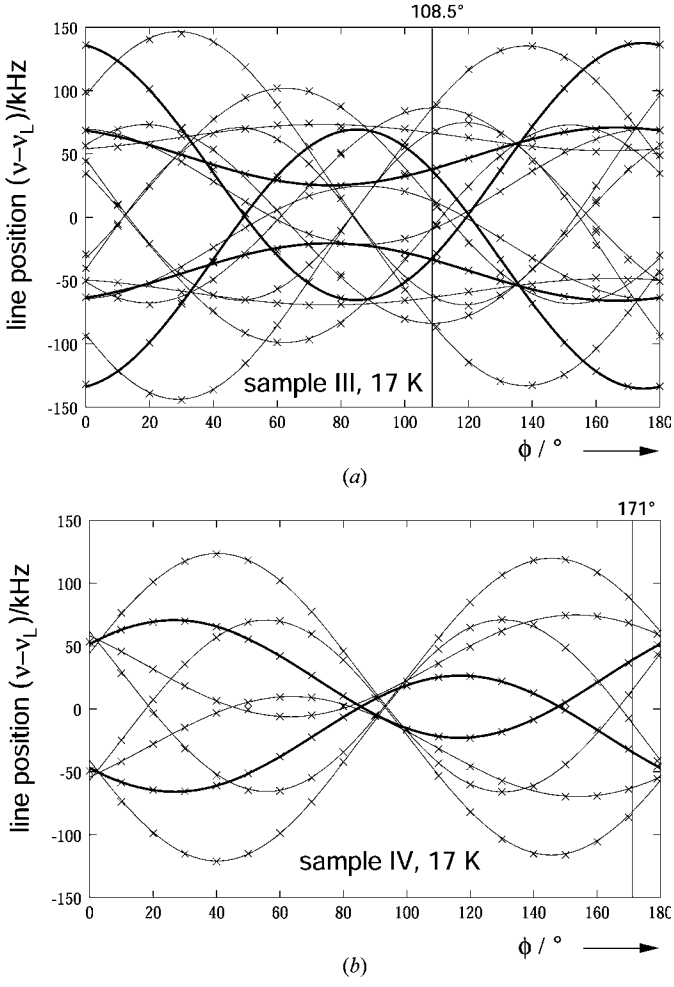


**Figure 4**
Rotation pattern of deuteron NMR line positions of samples III (*a*) and IV (*b*). The experimental data are connected by cosine curves. Those of the deuterons in the preferred sites 4 and 4′ are highlighted. For sample III, the path of **B** crosses the monoclinic plane at $\phi = 108.5^\circ$; this is indicated by a vertical line. The same orientation of **B** is encountered for sample IV at $\phi = 171^\circ$, also marked by a vertical line.

In the rotation pattern of that sample (Fig. 4*a*), there is one value of $\phi$ for which all traces cross pairwise (this occurs at $\phi = 108.5^\circ$). For this precisely locateable value of $\phi$, which we choose as $\phi^{\rm III}_{\rm ref}$, **B** lies in the monoclinic plane of the crystal. The pairs of traces that cross arise from pairs of deuterons related by $2_1$ axes. In Fig. 4, the traces corresponding to the deuterons in the preferred sites 4 and 4′ are highlighted. The information in Fig. 4(*a*) is again sufficient for a determination of the **Q** tensors of the respective deuterons. The (preliminary) knowledge of these tensors enables us (i) to find the rotation angle $\phi$ (=: $\phi^{\rm IV}_{\rm ref}$) in Fig. 4(*b*) for which **B** is oriented in the same direction relative to sample IV as is **B** relative to sample III for $\phi = \phi^{\rm III}_{\rm ref}$, and (ii) to assign the traces in rotation pattern IV to the same deuterons to which *pairs* of traces were assigned in rotation pattern III. This allows us to incorporate the information from both sample III and sample IV in the final fitting procedure and thus, by increasing the redundancy, to improve the accuracy. However, as for the fully deuterated sample II, we obtain equally good results in terms of the standard deviations if, in the fitting procedure, we reverse the sense of rotation of crystals III and IV simultaneously. In terms of the preferred bond directions $\mathbf{b}_4(\vartheta, \varphi)$ and $\mathbf{b}'_4(\vartheta', \varphi')$, the two solutions are:

$(\vartheta, \varphi) = (130.0^\circ, 105.9^\circ)$, $(\vartheta', \varphi') = (50.0^\circ, 74.1^\circ)$ for $\mathbf{d}^{\rm III}_{\rm rot} = (62.2^\circ, 43.7^\circ)$, $\mathbf{d}^{\rm IV}_{\rm rot} = -\mathbf{b}$; and

$(\vartheta_{\rm r}, \varphi_{\rm r}) = (90.1^\circ, 132.5^\circ)$, $(\vartheta'_{\rm r}, \varphi'_{\rm r}) = (89.9^\circ, 47.5^\circ)$ for $\mathbf{d}^{\rm III}_{\rm r,rot} = -\mathbf{d}^{\rm III}_{\rm rot}$, $\mathbf{d}^{\rm IV}_{\rm r,rot} = +\mathbf{b}$.

By comparing these results with those from sample II (and I), it is now perfectly clear that the sense of the rotation axes of all samples must be as indicated in Table 1. The hypothesis of reversed axes leads to a contradiction. We stress that by comparing the 17 K rotation pattern of the sparsely deuterated crystal IV with that of the fully deuterated crystal I (either at $T = 44$ K, not shown, or at 13 K, shown in Fig. 5) it is

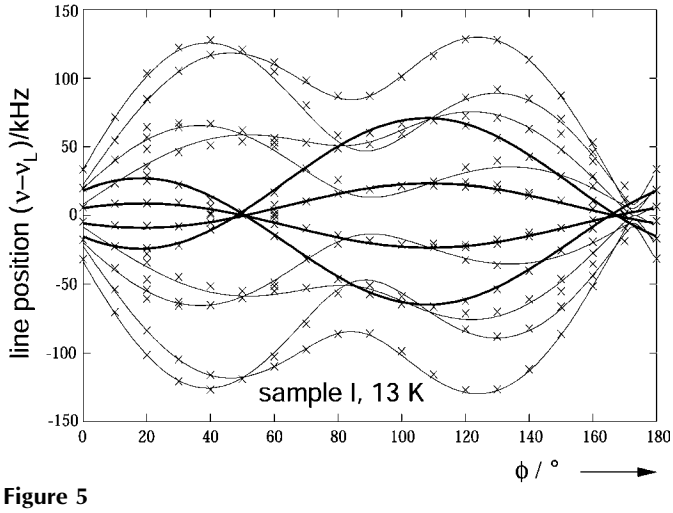


**Figure 5**
Rotation pattern of deuteron NMR line positions of sample I, $T = 13$ K. The (highlighted) curves connecting the data from the localized deuteron in the preferred site 4 and those from the $\beta$-lines of the remaining three tunnelling deuterons are cosine curves; those connecting the data from the $\alpha$- and $2\alpha$-lines of the tunnelling deuterons obey expressions that are more complicated [see Detken *et al.* (1995)].

**Table 2**
Deuteron quadrupole-coupling tensors **Q** in ammonium persulphate.

| Deuteron site | Principal value† (kHz) | Principal direction‡§ | |
|---|---|---|---|
| | | $\vartheta$ (°) | $\varphi$ (°) |
| 1 | −138.0 | 42.4 | 259.7 |
| | −135.0 | 142.1 | 250.5 |
| | +273.0 | **94.6** | **344.7** |
| 2 | −141.4 | 110.7 | 121.5 |
| | −135.2 | 89.3 | 211.2 |
| | +276.6 | **20.7** | **119.3** |
| 3 | −147.8 | 38.3 | 309.2 |
| | −143.1 | 54.0 | 152.4 |
| | +290.9 | **101.4** | **234.0** |
| 4 | −137.6 | 53.5 | 54.4 |
| | −135.1 | 118.8 | 348.4 |
| | +272.7 | **130.0** | **105.9** |

† Estimated errors ±1.5 kHz. ‡ Polar angles in the SO frame with $x \parallel \mathbf{a}$, $y \parallel \mathbf{b}$, $z \parallel \mathbf{c}^*$. § Unique principal directions in bold. These directions can be identified with the respective $\overrightarrow{\mathrm{N-D}}_i$ bond directions $\mathbf{b}_i$. Estimated errors ±0.3° (solid angle).

immediately evident which pair of traces in Fig. 4(*b*) must be assigned to the deuteron in the previously defined (preferred) site 4. We also stress that the deuteron NMR data allow for internal checks of the optically determined (unsigned) rotation axes. The number of doublets observed from samples I and IV confirms that the rotation axes of those samples must be parallel to the monoclinic crystal axis **b**. As regards the rotation axes $\mathbf{d}_{\rm rot}^{\rm II}$ and $\mathbf{d}_{\rm rot}^{\rm III}$ of samples II and III, at least the angle subtended by them with **b** can be verified: any attempt to change $<(\mathbf{d}_{\rm rot}^{\rm II}, \mathbf{b})$ or $<(\mathbf{d}_{\rm rot}^{\rm III}, \mathbf{b})$ leads to a dramatic deterioration of the quality of the fits. On the other hand, the separate fits of the data of samples I, II and of III, IV are insensitive to whether or not the projections of $\mathbf{d}_{\rm rot}^{\rm II}$ and $\mathbf{d}_{\rm rot}^{\rm III}$ onto the monoclinic crystal plane are correct. In this respect, we must trust the results of the optical orientation of the sample crystals. However, the fact that samples I, II and III, IV gave, within narrow limits, the same results for $\mathbf{b}_4$ and $\mathbf{b}_4'$ is strong evidence that these projections were indeed found correctly.

The quadrupole-coupling tensors of all deuterons in APS finally obtained from the 17 K rotation patterns of samples III and IV are listed in terms of their principal values and principal directions in Table 2. Note that all four **Q** tensors are nearly axially symmetric and thus do possess *unique* principal directions that we may identify with the N—D bond directions $\mathbf{b}_1$–$\mathbf{b}_4$.

The fitting procedure produces for each pair of monoclinic symmetry-related deuterons two **Q** tensors that are related by a twofold rotation. If we repeat the procedure for all four pairs of related deuterons, as we do in the present case, we cannot, without bringing into play an additional idea, sort the **Q** tensors and the corresponding deuterons into sets that belong to a common N atom. Remember, there are four N atoms in the unit cell. By their very nature, the principal directions come without 'point' and 'tail'. When compiling Table 2 we selected the tensors and the orientations of the unique principal directions such that the respective deuterons all belong to the same N atom and such that the unique principal directions all correspond to $\overrightarrow{\mathrm{N-D}}$ bond directions. The basis ('additional idea') of the selection is that the $\overrightarrow{\mathrm{N-D}}$ bond directions should conform at least approximately to tetrahedral symmetry. The angles subtended by the unique principal directions listed in Table 2 are all $109.4^\circ \pm 0.7^\circ$ and thus satisfy this condition with remarkable precision.

Before finally locating the deuterons in APS, we briefly discuss the rotation pattern of the fully deuterated sample I shown in Fig. 5. While the curves fitted to the data points from the $\beta$-lines and from the immobile deuteron in the preferred site 4 are cosine curves of the same type as all the curves in Figs. 3 and 4, the curves connecting the $\alpha$ and $2\alpha$ data points are obviously different. The rather complicated theoretical expression for these curves was derived for the NMR resonances of tunnelling $-CD_3$ groups (Detken *et al.*, 1995). The curves included in Fig. 5 are obviously good fits to the experimental data. The crucial fitting parameter allows us to find the rotation angle $\phi$ for which **B** and the equilibrium bond direction of one of the three uniaxially tunnelling deuterons span a plane $p$ that is perpendicular to the plane in which the three tunnelling deuterons lie. That latter plane is perpendicular to the (known) preferred bond direction. Knowledge of the plane $p$ and of the preferred bond direction, and invoking tetrahedral symmetry of the $ND_4^+$ ion, fully specifies the orientation of that group. The details of the procedure are described by Schmidt (1999). The result coincides closely with that derived in the more direct way described above from the deuteron NMR data of the sparsely deuterated APS samples III and IV.

Next, we turn to the length of the N—D bonds. On the one hand, it is well justified to resort to the standard N—H bond length, $r_{\rm NH} = 1.054$ Å (Ozaki, 1987); on the other, we can again draw on deuteron NMR. As mentioned above, the outermost doublet of the $\phi = 175^\circ$ spectrum in Fig. 2 shows a well resolved fine structure. An enlargement of the right-hand component of this doublet (assigned to the deuteron in site 4) is reproduced in Fig. 6. The fine structure arises from the proton–deuteron and nitrogen-14–deuteron magnetic dipole–

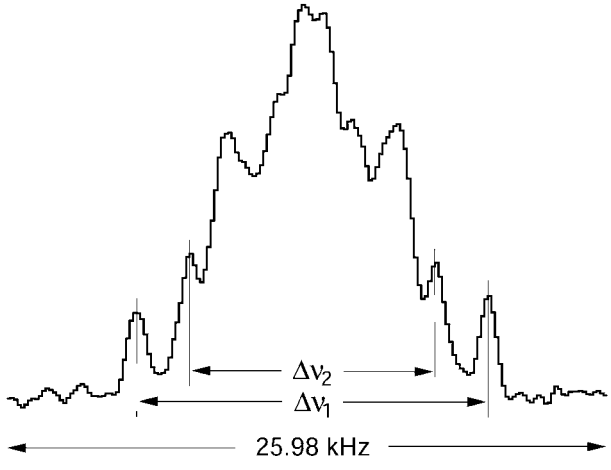


**Figure 6**
Detail of the high-frequency (right-hand) component of the outermost doublet of the $\phi = 175^\circ$ spectrum in Fig. 2 with definition of $\Delta\nu_1$ and $\Delta\nu_2$. The digital resolution is 152.85 Hz.

dipole interactions from within the $NDH_3^+$ ion. The strengths of these interactions,

$$d_{HD} = (\mu_0/4\pi^2)\hbar\gamma_H\gamma_D r_{HD}^{-3}\sum_{i=1}^{3}(1 - 3\cos^2\theta_{H_iD})/2 \qquad (2)$$

and

$$d_{ND} = (\mu_0/4\pi^2)\hbar\gamma_N\gamma_D r_{ND}^{-3}(1 - 3\cos^2\theta_{ND})/2, \qquad (3)$$

depend, apart from fundamental ($\hbar$, $\mu_0$) and nuclear (gyromagnetic ratios $\gamma_H$, $\gamma_D$, $\gamma_N$) constants, only on the (by now) known angles $\theta_{H_iD} = <(\mathbf{B}, \mathbf{r}_{H_iD})$ and $\theta_{ND} = <(\mathbf{B}, \mathbf{r}_{ND})$ and on the internuclear distances $r_{H_iD}$ and $r_{ND}$ in which we are interested. For tetrahedral symmetry of the ammonium ion and assuming $r_{ND} = r_{NH_i}$ we have, trivially, $r_{HD} = 2(2/3)^{1/2}r_{ND}$ and, more importantly,

$$-\sum_{i=1}^{3}(1 - 3\cos^2\theta_{H_iD})/2 = (1 - 3\cos^2\theta_{ND})/2, \qquad (4)$$

irrespective of the direction of **B**. In general, the fine structure of the deuteron resonance depends also on the dynamics of the protons in the $NDH_3^+$ ion, *i.e.* on whether they are static, are reorienting stochastically about the stationary N—D bond or are undergoing rotational tunnelling. In a follow-up paper we will demonstrate that, for $T \lesssim 25$ K, the protons of $NDH_3^+$ groups in APS undergo simultaneously fast rotational tunnelling and fast stochastic reorientations, provided that the deuteron is in the preferred site 4. Note that rotational tunnelling *plus* simultaneous stochastic reorientations *is* a dynamic option for an $-NH_3$ group (Szymański *et al.*, 1996). What is crucial in the present context is that the fine structure becomes independent of any dynamics of the protons if the magnetic field **B** is parallel to the (stationary) N—D bond. For the $\phi = 175^\circ$ spectrum in Fig. 2, this situation is closely encountered for deuteron 4, the angle subtended by **B** and $r_{ND}$ being $\theta_{ND} = 3^\circ$. The analysis of the dipole–dipole interactions within the $NDH_3^+$ ion then becomes straightforward and tells us that the splittings $\Delta\nu_1$ and $\Delta\nu_2$ of the two outermost doublets in Fig. 6 are related to $d_{HD}$ and $d_{ND}$ by

$$|\Delta\nu_1| = |\Delta\nu_2| + 2|d_{ND}| \qquad (5)$$

and

$$|\Delta\nu_2| = (3/2)|d_{HD}|. \qquad (6)$$

From Fig. 6 we take $|\Delta\nu_1| = 15.27\ (7)$ kHz and $|\Delta\nu_2| = 10.67\ (7)$ kHz, and by inserting these values together with $\theta_{ND} = 3^\circ$ into equations (2), (3), (5) and (6) and making use of (4), we can solve for $r_{ND}$ and $r_{HD}$. In this way, we obtain directly $r_{ND} = 1.049$ Å and $r_{HD} = 1.729$ Å, and from this latter value we obtain indirectly for the N—D distance $(1/2)(3/2)^{1/2}r_{HD} = 1.0585$ Å. The digital resolution of the spectrum in Fig. 6 is 152.85 Hz; the errors $\delta\Delta\nu_1$ and $\delta\Delta\nu_2$ are, nevertheless, considerably smaller, say $\delta\Delta\nu_1 = \pm 50$ Hz and, because of inferior resolution, $\delta\Delta\nu_2 = \pm 70$ Hz corresponding to errors of $r_{HD}$ and $r_{ND}$ of $\pm 0.005$ Å and $\pm 0.007$ Å, respectively. All these numbers confirm with remarkable precision that the standard N—H bond length is valid in APS and, within the stated error limits, it is also valid for the N—D bond length.

**Table 3**
Comparison of experimental values of $Q_{ZZ}$ with those calculated using (7) for the four candidate assignments of bundles of bond vectors to nitrogen atom N.

Assignment $\mathbf{b}_i$ is strongly favored, particularly if site 3, whose deuteron evidently is not involved in a hydrogen bond, is excluded from the comparison.

| | | Deuteron site | | | |
|---|---|---|---|---|---|
| Assignment to N | | 1 | 2 | 3 | 4 |
| | $r_{D\cdots O}$ (Å) | 1.9271 | 1.9906 | 2.2332 | 1.9113 |
| $\mathbf{b}_i$ | <(NDO) (°) | 153.8 | 142.3 | 129.0 | 175.1 |
| | $Q_{ZZ}$ calculated (kHz) | 272.2 | 282.1 | 310.5 | 269.5 |
| | $Q_{ZZ}$ experimental (kHz) | 272.96 | 276.58 | 290.90 | 272.76 |
| $\bar{\mathbf{b}}_i$ | $Q_{ZZ}$ calculated (kHz) | 317.5 | 314.8 | 283.6 | 300.2 |
| $\mathbf{b}'_i$ | $Q_{ZZ}$ calculated (kHz) | 316.7 | 311.1 | 318.8 | 305.1 |
| $\bar{\mathbf{b}}'_i$ | $Q_{ZZ}$ calculated (kHz) | 283.8 | 290.8 | 302.1 | 278.2 |

At this stage, we have found a bundle of four $\overrightarrow{N-D}$ bond vectors $\mathbf{b}_i$, $i = 1, \ldots, 4$, of known directions (see highlighted entries in Table 2) and lengths (we take the average 1.054 Å of 1.049 Å and 1.0585 Å), and we know they have a common origin. The crystal symmetry implies that there are three more such bundles to be designated $\bar{\mathbf{b}}_i$, $\mathbf{b}'_i$ and $\bar{\mathbf{b}}'_i$, the bar indicating inversion, the prime, as before, monoclinic symmetry-related. What we do not know yet is which of these bundles is to be assigned to, for example, the N atom whose fractionals are listed in Table 1 of Sivertsen & Sørum (1969). So, the last step of our deuteron NMR location of the H atoms in APS is to assign the proper bundle of $\overrightarrow{N-D}$ bond vectors to this N atom.

To solve this assignment problem, we draw on the empirical relation

$$Q_{ZZ} = 379.5 - \left(768/[r_{D\cdots O}]^3\right), \qquad (7)$$

which relates the largest principal value, $Q_{ZZ}$ (in kHz), of the **Q** tensor of a deuteron in an N—D···O hydrogen bond to the D···O internuclear distance (Blinc, 1976). Of course, (7) is not quantitative but gives only an estimate of $Q_{ZZ}$. It does not take into account, for example, how much the hydrogen bond is bent. It shows: strong hydrogen bond (short D···O distance) $\Longrightarrow$ small $Q_{ZZ}$; weak or no hydrogen bond (large D···O distance) $\Longrightarrow$ large $Q_{ZZ}$.

We tested all four candidate assignments. Each test consisted of (i) finding for each hypothetical deuteron position the distance $r_{D\cdots O}$ to the *nearest* O atom, (ii) calculating the NDO bond angle <(NDO) as a guide to judge whether or not a hydrogen bond is likely to be formed, and (iii) inserting $r_{D\cdots O}$ into (7) to obtain a 'theoretical' estimate of $Q_{ZZ}$. In Table 3 we show the results for assigning the bundle $\mathbf{b}_i$ to N and, in an abbreviated form, those for the other candidate assignments. A look at this table will quickly convince the reader that the assignments $\bar{\mathbf{b}}_i$ and $\mathbf{b}'_i$ can safely be rejected. The best agreement between calculated and experimental $Q_{ZZ}$ is obtained for assignment $\mathbf{b}_i$, but assignment $\bar{\mathbf{b}}'_i$ must also be considered seriously. The latter is better with regard to site 3. This preference is, however, largely immaterial, because for either

**Table 4**
Equilibrium positions of the hydrogen nuclei in APS.

$\Delta f_{\alpha,i}$ express the $\overrightarrow{\mathrm{N-D}}_i$ bond vectors measured by deuteron NMR at 17 K in terms of the room-temperature unit-cell parameters $a$, $b$, $c$ and $\beta$ as given by Sivertsen & Sørum (1969). The fractionals $f_{\alpha,i}$ of the H atoms are obtained by adding $\Delta f_{\alpha,i}$ to the fractionals of the N atom as given by these authors. The assumptions underlying this procedure are discussed in the text.

| Site | $\Delta f_a$† | $\Delta f_b$ | $\Delta f_c$ | $f_a$ | $f_b$ | $f_c$ |
|---|---|---|---|---|---|---|
| 1 | 0.1179 | −0.0350 | −0.0137 | 0.2078 | 0.8489 | 0.2194 |
| 2 | 0.1268 | 0.0410 | 0.1613 | 0.2166 | 0.9249 | 0.3944 |
| 3 | −0.1101 | −0.1053 | −0.0340 | −0.0202 | 0.7786 | 0.1991 |
| 4 | −0.1318 | 0.0979 | −0.1109 | −0.0419 | 0.9818 | 0.1222 |

† The uncertainty of $\Delta f_\alpha$ is 0.0008.

assignment the deuteron in site 3 can hardly be said to form a hydrogen bond and therefore (7) cannot be expected to work. The 'large' experimental value of $Q_{ZZ}$ of the deuteron in site 3, 290.8 kHz, supports the non-hydrogen-bond hypothesis. All the other entries in Table 3 speak strongly in favor of assignment $\mathbf{b}_i$. Unlike assignment $\bar{\mathbf{b}}'_i$, it suggests, as does the experiment, that the deuterons in sites 1 and 4 form hydrogen bonds of comparable strength. Again, in agreement with the experiment, the assignment $\mathbf{b}_i$ suggests, unlike that for $\bar{\mathbf{b}}'_i$, that the deuteron in site 2 is also involved in a hydrogen bond, albeit in a weaker one than the deuterons in sites 1 and 4.

Therefore, we propose that it is the bundle $\mathbf{b}_i$ of $\overrightarrow{\mathrm{N-D}}$ bond vectors that must be assigned to the nitrogen atom N. The strongest and final argument for the correctness of this proposition is that it is confirmed by the X-ray diffraction results (see below).

The bundle $\mathbf{b}_i$ of $\overrightarrow{\mathrm{N-D}}$ bond vectors can be represented by a set of incremental fractionals $\Delta f_{\alpha,i}$, $\alpha = a, b, c$; $i = 1, \ldots, 4$. This set is given in Table 4. It applies to $T = 17$ K and expresses $\mathbf{b}_i$ in terms of the room-temperature lattice parameters $a$, $b$, $c$ and $\beta$ as given by Sivertsen & Sørum (1969). Added to the fractionals of the N atoms, $\Delta f_{\alpha,i}$ give the fractionals $f_{\alpha,i}$ of the H atoms in APS. Assuming that the directions of $\mathbf{b}_i$ are the same at room temperature as they are at 17 K (the distances $r_{\mathrm{ND}}$ do not change significantly) and using for the N-atom position the data of Sivertsen & Sørum (1969), we obtain the room-temperature equilibrium positions of the H atoms in APS. They are also given in Table 4 and complete the list of fractionals in Table 1 of Sivertsen & Sørum (1969). Note that they refer to the *nuclei* of the H atoms. A projection of the immediate neighborhood of an $ND_4^+$ ion in APS onto the monoclinic crystal plane is shown in Fig. 7.

## 5. Discussion

All H atoms in APS have several O atoms nearby. Given the set of N—D bond directions (see Table 2), the actual structure (*i.e.* the assignment of $\mathbf{b}_i$ to N) is that which minimizes the D···O distances under the constraint of almost perfect tetrahedral geometry of the ammonium ion. Because short D···O distances mean strong N—D···O hydrogen bonds, the structure thus reflects the strongest possible orientational fixation of the ion. This fixation is, nevertheless, weak. It does not prevent the $ND_4^+$ ions reorienting frequently at temperatures as low as 70 K, *cf.* the discussion of Fig. 1. The shortest and most stretched, and therefore strongest, hydrogen bond is formed by the deuteron in site 4 (see Fig. 7). If any of the deuterons is to play a special dynamic role, it is no surprise that it is this deuteron. It is the only one of the $ND_4^+$ ions that becomes localized at low temperatures, and its bond becomes the primary rotational-tunnelling axis. Rotational tunnelling about other axes (other N—D bonds) implies breaking the 'strong' hydrogen bond of the deuteron in site 4 with the natural consequence that any secondary tunnelling frequency must be small, as it is found to be in the NMR experiments. For $NH_3D^+$ ions, the special role of site 4 is revealed, apart from the dynamics of the protons, by isotopic ordering: at low temperatures, the deuteron of such ions goes preferentially into that site. As mentioned in the discussion of Fig. 2, the three other sites are not perfectly equivalent. Site 1 is slightly more populated by deuterons than are sites 2 and 3. This observation is in line with our conclusion that the deuteron in site 4 and that in site 1 both form a hydrogen bond of significant strength.

## 6. X-ray diffraction

To verify the results from the deuteron NMR experiments we carried out an X-ray analysis of perdeuterated APS. Because we are primarily interested in the positions of the H atoms, the main data set was collected at 118 K to reduce thermal motions of the H atoms as much as possible. Preliminary data were also collected at ambient temperature. A Nonius

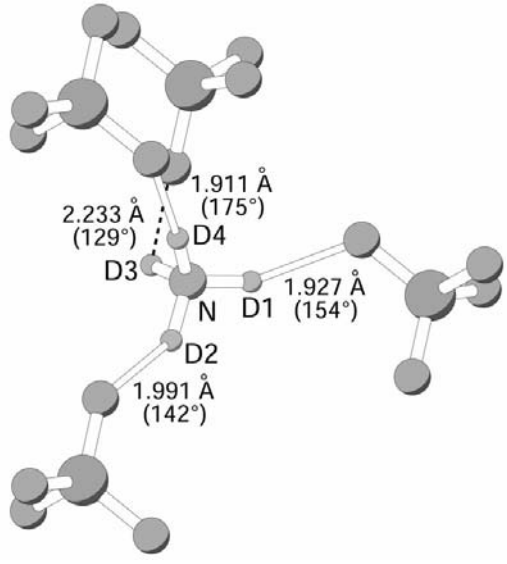


**Figure 7**
View of the neighborhood of an $ND_4^+$ ion in APS, projection along **b**. The equilibrium deuteron sites are labeled. Site 4 is the preferred one. The (non-hydrogen-bonded) O atom nearest to the deuteron in equilibrium site 3 is connected to that deuteron by a dashed line. Note that all O atoms with short D—O contacts belong to different $SO_4$ tetrahedra.

**Table 5**
Experimental details.

| | APS |
|---|---|
| Crystal data | |
| Chemical formula | $(SO_4)_2(NH_4)_2$ |
| Chemical formula weight | 228.2 |
| Cell setting, space group | Monoclinic, $P2_1/n$ |
| $a, b, c$ (Å) | 6.1340 (2), 7.9324 (3), 7.7541 (3) |
| $\beta$ (°) | 94.966 (1) |
| $V$ (Å$^3$) | 375.88 (2) |
| $Z$ | 2 |
| $D_x$ (Mg m$^{-3}$) | 2.016 |
| Radiation type | Mo $K\alpha$ |
| No. of reflections for cell parameters | 786 |
| $\theta$ range (°) | 5.1–27.9 |
| $\mu$ (mm$^{-1}$) | 0.728 |
| Temperature (K) | 118 (2) |
| Crystal form, color | Fragment, colorless |
| Crystal size (mm) | 0.32 × 0.20 × 0.20 |
| $F(000)$ | 236 |
| Data collection | |
| Diffractometer | Nonius KappaCCD diffractometer |
| Data collection method | $\varphi$ and $\omega$ scans |
| No. of measured, independent and observed reflections | 1393, 791, 768 |
| Variables | 71 |
| Criterion for observed reflections | $I > 2\sigma(I)$ |
| $R_{int}$ | 0.024 |
| $\theta_{max}$ (°) | 27.86 |
| Range of $h, k, l$ | $-8 \rightarrow h \rightarrow 8$<br>$-10 \rightarrow k \rightarrow 10$<br>$-10 \rightarrow l \rightarrow 10$ |
| Refinement | |
| Refinement on | $F^2$ |
| $R[F^2>2\sigma(F^2)]$, $wR(F^2)$, $S$ | 0.028, 0.069, 1.067 |
| No. of reflections and parameters used in refinement | 791, 71 |
| H-atom treatment | Refined isotropic |
| Weighting scheme | $w = 1/[\sigma^2(F_o^2) + (0.0151P)^2 + 0.2285P]$ where $P = (F_o^2 + 2F_c^2)/3$ |
| $(\Delta/\sigma)_{max}$ | 0.002 |
| $\Delta\rho_{max}$, $\Delta\rho_{min}$ (e Å$^{-3}$) | 0.252, −0.303 |

Computer programs used: *Collect Package* (Bruker Nonius, 1999), *SHELXS*97 (Sheldrick, 1997), *SHELXL*97 (Sheldrick, 1997).

KappaCCD diffractometer (Mo $K\alpha$ radiation, graphite monochromator) equipped with a nitrogen low-temperature unit was used. Data collection and reduction were performed with the *Collect* package (Bruker Nonius, 1999). Structure solution succeeded with direct methods (Sheldrick, 1997). The structural parameters of the non-H atoms were refined anisotropically according to a full-matrix least-squares technique ($F^2$). All deuterons were refined isotropically as H atoms. Refinement was carried out with *SHELXL* (Sheldrick, 1997). The complete refinement procedure was carried out in the space group $P2_1/n$. Subsequently the data were transformed to $P2_1/c$ to ease comparison with the NMR experiments.

Table 5 contains the crystallographic data and details of the refinement procedure; in Table 6 we list the atom positions.[1]

[1] Supplementary data for this paper are available from the IUCr electronic archives (Reference: SN0024). Services for accessing these data are described at the back of the journal.

**Table 6**
Atomic coordinates and isotropic displacement parameters $U$(eq) in space group $P2_1/c$.

The labeling of the O atoms follows Sivertsen & Sørum (1969).

| | $x$ | $y$ | $z$ | $U$(eq) |
|---|---|---|---|---|
| S | 0.42360 (6) | 0.35461 (4) | 0.28615 (4) | 0.0135 (2) |
| N | 0.0805 (2) | 0.8853 (2) | 0.2287 (2) | 0.0172 (3) |
| O1 | 0.4052 (2) | 0.5187 (1) | 0.3817 (1) | 0.0212 (3) |
| O2 | 0.3413 (2) | 0.2109 (1) | 0.3157 (2) | 0.0242 (3) |
| O3 | 0.2402 (2) | 0.4108 (1) | 0.0649 (1) | 0.0198 (2) |
| O4 | 0.7009 (2) | 0.3482 (1) | 0.4167 (2) | 0.0192 (2) |
| D1 | 0.179 (4) | 0.861 (2) | 0.218 (4) | 0.035 (6) |
| D2 | 0.170 (5) | 0.909 (3) | 0.351 (4) | 0.038 (5) |
| D3 | −0.010 (5) | 0.799 (3) | 0.189 (4) | 0.051 (7) |
| D4 | −0.027 (4) | 0.964 (3) | 0.142 (3) | 0.023 (4) |

N—D bond directions expressed by polar angles $\vartheta, \varphi$ in the SO frame.

| | $\vartheta$ (°) | $\varphi$ (°) | $\delta$ (°)† |
|---|---|---|---|
| N—D1 | 94.3 | 347.1 | 2.4 |
| N—D2 | 19.7 | 135.2 | 5.6 |
| N—D3 | 106.9 | 238.8 | 7.2 |
| N—D4 | 128.8 | 108.4 | 2.3 |

† Difference of solid angle to bond directions found by deuteron NMR, *cf.* Table 2.

**Table 7**
Listing of the hydrogen bonds drawn in Fig. 8.

| O···D (Å) | | N···O (Å) | | <(N—D···O) (°) | |
|---|---|---|---|---|---|
| O4···D1 | 2.10 | N···O4 | 2.901 | N—D1···O4 | 160.0 |
| O2···D2 | 2.18 | N···O2 | 2.873 | N—D2···O2 | 145.9 |
| O4···D2 | 2.57 | N···O4 | 2.979 | N—D2···O4 | 113.8 |
| O2···D3 | 2.28 | N···O2 | 2.978 | N—D3···O2 | 142.8 |
| O4···D4 | 2.09 | N···O4 | 2.929 | N—D4···O4 | 177.6 |

Those of the S, O and N atoms confirm the structure of APS as found by Sivertsen & Sørum (1969), but the data are considerably more precise. Most important in the present context is that well defined H-atom positions could be identified. Basically, they confirm the deuteron positions found in the NMR part of this work; in particular, they confirm the correctness of the assignment of the bundle $\mathbf{b}_i$ of N—D bond vectors to the nitrogen atom N in the unit cell, *cf.* Table 3. When comparing the hydrogen positions in Tables 4 and 6, one should bear in mind that the NMR data refer to the *nuclei* while those from the X-ray diffraction refer to the centers of the *electron* clouds. To ease the comparison, we also list in Table 6 the N—D bond directions implied by the X-ray N and D positions. As can be seen, these bond directions agree remarkably well with those derived from deuteron NMR (see Table 2).

The X-ray study reveals that crystals of APS form a complex network of hydrogen bonds between alternate layers of persulphate and ammonium ions. This is shown in Fig. 8, wherein the O···D bridge bonds are indicated as fragmented lines. The $S_2O_8^{2-}$ and $ND_4^+$ ions, respectively, are arranged in rows parallel to *c*. Table 7 lists all hydrogen contacts drawn in Fig. 8. Note that the O—$D_i$ distances in this table are all longer than in Table 3, which is natural because of the necessary

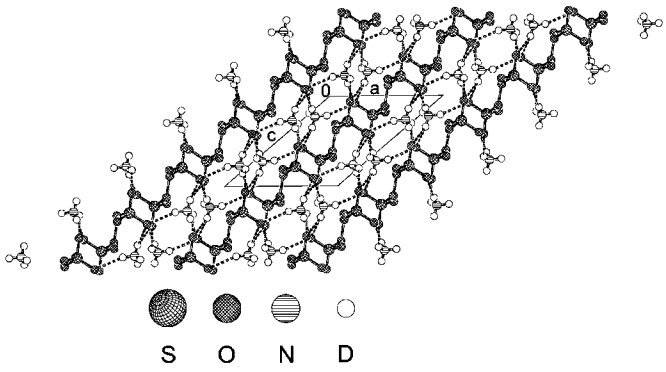


**Figure 8**
Packing arrangement of APS in the space group $P2_1/c$. View along the crystallographic *b* axis. Short D···O contacts (below 2.6 Å) are indicated as fragmented bonds.

distinction between the nucleus and center-of-electron positions. However, the X-ray and NMR results agree in that the deuteron 4 forms the shortest and most linear hydrogen bond, followed by deuteron 1. Deuteron 2 forms a bifurcated hydrogen bond, with the second O atom being, however, rather far away (2.57 Å). The bifurcated hydrogen bond of deuteron 2 may explain why the N—D2 bond, rather than the N—D1 bond with the *shorter* D1···O distance, becomes the axis of secondary tunnelling at low temperatures, *i.e.* $T < 25$ K (Olejniczak *et al.*, 2002). The ambient-temperature X-ray results indicate that the H-atom equilibrium sites in APS do not change significantly all the way from 17 K to 295 K despite dramatic changes that take place in the dynamics of the $ND_4^+$ ions.

We thank one of the referees of the first version of this paper for drawing our attention to the problem of combining low- and room-temperature structural information. ZTL gratefully acknowledges an Alexander von Humboldt fellowship for an extended stay at the MPI in Heidelberg in the fall of 1998. Participation of ZTL and ZO in this project was partially supported by the State Committee for Scientific Research (Poland), Grant No. 2 P03B 07415.

## References

Bernhard, T. & Haeberlen, U. (1991). *Chem. Phys. Lett.* **186**, 307–312.
Blinc, R. (1976). *The Hydrogen Bond*, edited by P. Schuster, G. Zundel & C. Sandorfy, pp. 831–887. Amsterdam: North-Holland. [Note that Blinc has written equation (7) in terms of the quadrupole coupling constant $QCC = 2Q_{ZZ}/3$.]
Bruker Nonius, B. V. (1999). *Collect Package.* Delft, The Netherlands.
Clough, S., Horsewill, A. J., Johnson, M. R., Mohammed, M. A. & Newton, T. (1991). *Chem. Phys.* **152**, 343–351.
Detken, A., Focke, P., Zimmermann, H., Haeberlen, U., Olejniczak, Z. & Lalowicz, Z. T. (1995). *Z. Naturforsch. Teil A*, **50**, 95–116.
Kankaanpää, M., Ylinen, E. E. & Punkkinen, M. (2001). *Solid State NMR*, **19**, 19–28.
Lalowicz, Z. T., Punkkinen, M., Vuorimäki, A. H., Ylinen, E. E., Detken, A. & Ingman, L. P. (1997). *Solid State NMR*, **8**, 89–107.
Lalowicz, Z. T., Werner, U. & Müller-Warmuth, W. (1988). *Z. Naturforsch. Teil A*, **43**, 219–227.
Mehring, M. (1976). *High Resolution NMR Spectroscopy in Solids*, edited by P. Diehl, E. Fluck & R. Kosfeld. Berlin/Heidelberg/New York: Springer-Verlag.
Olejniczak, Z., Lalowicz, Z. T., Schmidt, T., Zimmermann, H., Haeberlen, U. & Schmitt, H. (2002). *J. Chem. Phys.* **116**, 10343–10355.
Ozaki, Y. (1987). *J. Phys. Soc. Jpn*, **56**, 825–826.
Schiebel, P., Papoular, R. J., Paulus, W., Zimmermann, H., Detken, A., Haeberlen, U. & Prandl, W. (1999). *Phys. Rev. Lett.* **83**, 975–978.
Schmidt, T. (1999). MSci thesis, Max-Planck-Institute für Medizinische Forschung, Heidelberg, Germany.
Schmitt, H., Zimmermann, H., Körner, O., Stumber, M., Meinel, C. & Haeberlen, U. (2001). *J. Magn. Reson.* **151**, 65–77.
Sheldrick, G. M. (1997). *SHELXS*97. *SHELXL*97. Institut für Anorganische Chemie der Universität, Göttingen, Germany.
Sivertsen, B. K. & Sørum, H. (1969). *Z. Kristallogr.* **130**, 449–460.
Szymański, S., Olejniczak, Z. & Haeberlen, U. (1996). *Physica B*, **226**, 161–163.
Tesche, B., Zimmermann, H., Poupko, R. & Haeberlen, U. (1993). *J. Magn. Reson.* A**104**, 68–77.
Zachariasen, W. H. & Mooney, R. C. L. (1934). *Z. Kristallogr.* **88**, 63–81.